THE JOURNAL OF PHYSICAL CHEMISTRY A

Article

Cite This: J. Phys. Chem. A 2019, 123, 2780−2788

pubs.acs.org/JPCA

Anomalous Intensities in the 2+1 REMPI Spectrum of the E $^1\Pi$−X $^1\Sigma^+$ Transition of CO

Published as part of The Journal of Physical Chemistry virtual special issue "Hanna Reisler Festschrift".

C. E. Gunthardt,[†] C. J. Wallace,[†] G. E. Hall,[‡] R. W. Field,[§] and S. W. North*[,†]

[†]Department of Chemistry, Texas A&M University, College Station, Texas 77843, United States

[‡]Chemistry Division, Brookhaven National Laboratory, Upton, New York 11973, United States

[§]Department of Chemistry, Massachusetts Institute of Technology, Cambridge, Massachusetts 02139, United States

ABSTRACT: We report on one-color experiments near 214 nm involving the photodissociation of jet-cooled OCS to produce high rotational states ($40 < J < 80$) of CO ($X\ ^1\Sigma^+$, $v = 0, 1$) which were then ionized by 2+1 resonance-enhanced multiphoton ionization via the E $^1\Pi$ state. The nominally forbidden Q-branch of the two-photon E $^1\Pi$−X $^1\Sigma^+$ transition is observed with intensity comparable to the allowed R-branch. The bright character of the high-J Q-branch lines can be described quantitatively as intensity borrowing due to mixing of the E $^1\Pi$ and C $^1\Sigma^+$ states, using J-dependent mixing coefficients extrapolated from the observed Λ-doubling in the lower rotational levels of the E state. In addition to the significant enhancement of Q-branch intensities above the values predicted by conventional two-photon line strengths for a $^1\Pi$−$^1\Sigma^+$ transition, the high-J lines of the R- and P-branches appear to be suppressed in intensity by approximately a factor of 3 compared to the unperturbed low-J line strengths, most likely due to perturbations associated with a $^1\Sigma^-$ state. The E-state rotational term values for $J < 80$, $v = 0$ derived from the present spectra agree within our measurement and calibration uncertainties with the extrapolations based on the molecular constants previously derived from rotational levels with $J < 50$. The E−X transition is attractive for future application to photodissociation dynamics and rotational polarization measurements of CO photofragments, with convenient access to state-selective probing on multiple rotational branches, which exhibit different sensitivity to fragment alignment.

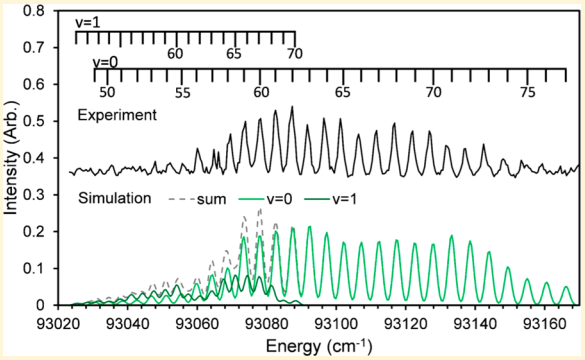

1. INTRODUCTION

Resonance-enhanced multiphoton ionization (REMPI) spectroscopy, combined with velocity-mapped ion imaging provides a powerful means of gaining insight into the photofragmentation dynamics of small molecules.[1−8] For the detection of CO photofragments, ionization using the 2+1 REMPI scheme via the B $^1\Sigma^+$−X $^1\Sigma^+$ transition near 230 nm or the C $^1\Sigma^+$−X $^1\Sigma^+$ transition near 217 nm have been used in previous studies.[4−7,9] As a two-photon $^1\Sigma^+$−$^1\Sigma^+$ transition, the intensity is primarily in the Q-branch, which is nearly insensitive to rotational polarization and photofragment vector correlations.[4] In order to assess rotational polarization effects with ion imaging, we consider the E $^1\Pi$−X $^1\Sigma^+$ 2+1 REMPI system.[10−13] Using this $^1\Pi$−$^1\Sigma^+$ transition, variations in the polarization-dependent ion images will be sensitive to the vector properties of the photodissociation, which can be extracted from multiple images acquired in different geometries and with different rotational branch transitions.[14]

The E $^1\Pi$ state of CO has been extensively studied over many years and is experimentally known from the one-photon absorption spectroscopy of the E $^1\Pi$−X $^1\Sigma^+$ system,[15−17] as well as from the E $^1\Pi$−A $^1\Pi$ and E $^1\Pi$−B $^1\Sigma^+$ emission spectra.[18,19] The E state is located above the dissociation energy of CO, and the competition between fluorescence and dissociation increasingly favors dissociation at higher vibrational levels of the E state.[16,20−22] The predissociation is presumed to occur through a J-independent, homogeneous electrostatic interaction with the continuum of the A $^1\Pi$ state[23] as well as through occasional local perturbations. The local perturbations are identified through shifted, weakened, or extra lines[12,18,24] and attributed to spin−orbit interactions of certain rotational levels of the E $^1\Pi$ state with nearby levels of the k $^3\Pi$ state.[18,22−25] Recent theoretical work[23,26−28] has identified Rydberg-valence interactions as being responsible for some of the unusual $^1\Pi$ levels higher in the VUV region, including the E state, which is depicted as the inner portion of an adiabatic double-well potential with E and E′ labels for the inner and outer wells, connected by an avoided crossing. Configuration interaction, mixing some valence E′ character into the

Received: January 4, 2019
Revised: February 17, 2019
Published: February 27, 2019

DOI: 10.1021/acs.jpca.9b00109
J. Phys. Chem. A 2019, 123, 2780−2788

primarily Rydberg E state, is invoked to mediate the indirect spin−orbit interaction with the k $^3\Pi$ levels.[23,25,28]

Predissociation rates from all low rotational levels of v = 0 in the E state are fast enough to give a dissociation yield of about 90% and to suppress the fluorescence lifetime to about 1 ns, without introducing perceptible broadening to the E−X (0−0) line spectra.[16,29] The predissociation rate is about 10 times faster in v = 1 levels of the E state, as confirmed by both direct time-domain fluorescence decay measurements[29] and high-resolution measurements of line broadening.[22] Dispersed fluorescence following electron impact excitation has been observed to include E−X, C−X, and B−X emissions.[21] The Q-branch of the E−X (0−0) band emission was found to be reduced to 63% of its expected value relative to P- and R-branch intensity, in a 330 K spectrum, assuming unperturbed Hönl−London factors for emission and no difference in the excitation or predissociation rates for the two Λ components of the E state. An enhanced predissociation rate was inferred that appeared independent of J, but faster for the f component than the e component. Such a J-independent, but Λ-selective interaction cannot occur from a $^1\Pi$ state. Indeed, in a subsequent direct time-resolved measurement, a lifetime of 912 ± 60 ps was reported for v = 0 of the E state,[29] independent of rotational temperature or rotational branch in a free-jet experiment with sufficient spectral resolution to separate rotational branches, but not individual rotational lines.

Numerous studies have explored the oscillator strengths, emission yields, and predissociation of CO states in the vacuum ultraviolet (VUV) energy region to model the astrophysical abundances, isotopic fractionation, and photophysics of CO in space environments.[16,20,21,30−32] High-resolution spectroscopic measurements of quasar backlit CO absorption, including the E−X system, shifted into the visible spectral region by large cosmological red shifts, have been used to assess the constancy of the proton-to-electron mass ratio over cosmological time scales.[33] A recent atlas of CO transitions in the VUV for astrophysical purposes summarizes the extensive spectroscopic work on the CO E state, along with many other nearby and potentially interacting states.[31] Some of the most informative features of these excited states come from measurements of perturbations.[34,35] They can be revealed by intensity irregularities, missing or extra lines, spectral shifts, line widths and lifetimes, and predissociation product state distributions.[36] The perturbations may be independent of J, increasing with J, or they may occur only for specific rotational levels, and for degenerate electronic states, they may occur for either or both Λ components, according to the mutually interacting states and the type of interaction. Variations among isotopomers can further help to characterize the states involved and mechanisms.[22,23,29] In most of these spectroscopic studies, the observed rotational states were limited to those substantially populated at or below room temperature, typically for $J < 20$, or in one case,[24] in deliberately heated samples, up to $J < 50$.

The E−X system of CO has also been observed by 2+1 REMPI spectroscopy[10−12,24] and found to be suitable for state-resolved probing of the CO X state.[37] For thermal samples of CO, the REMPI intensities were found to closely match the conventional line strengths for O-, P-, R-, and S-branches in the E−X origin band, after accounting for a slight suppression of the CO^+ signal at higher rotational states, attributed to secondary photodissociation of CO^+.[2,11] A weak, unresolved Q-branch bandhead was observed, and as expected, no high-J Q-branch lines were observed or reported. A slight suppression of all S-branch lines was reported, compared to the other branches observed in a thermal CO sample.[11] In the present report, we find dramatically different behavior in the very high rotational states produced in the UV photodissociation of OCS, as the J-dependent state mixing becomes increasingly important.

Previous work from this laboratory[1] reported on the photodissociation of OCS followed by probing CO in the 214 nm region, through the E state, in a one-color experiment. At this excitation energy OCS photodissociation produces S(^{1}D) and almost exclusively very high rotational states of CO ($40 < J < 80$) in vibrational states v = 0 and v = 1. The E−X spectrum for these hot rotational states was observed and used to characterize the rotational distribution, primarily using the S-branch lines. The P- and O-branches of the E−X band display congested band heads at these high rotational levels and are not particularly useful for state-resolved measurements (see Figure 2 below). An extra set of lines was observed in the CO spectrum that is not predicted from either v = 0 or v = 1 of CO between 214.5 and 215 nm that we now attribute to Q-branch lines from high rotational states of both v = 0 and v = 1 of the CO ground state, despite the rapidly decreasing two-photon line strength for Q-branch lines expected at increasing J for a $^1\Pi-{}^1\Sigma^+$ transition.[38]

The peculiar property of OCS photodissociation that channels enormous energy into CO photofragment rotation through direct dissociation in a linear-to-bent transition opens wide an experimental window to observe J-dependent state mixing and perturbations that are weak and hard to characterize in cold or thermal samples. While by no means a universal method, this combination of photolytic preparation with prompt spectroscopic probing[39] can address some of the same properties of superexcited rotational levels that have recently been the subjects of investigation in optical centrifuge studies.[40−43]

Section 2 is a brief description of the experimental details. Section 3.1 is an overview of the CO E−X spectrum from the one-color OCS experiment. The additional lines observed are confirmed in section 3.2 to be high-J Q-branch transitions based on the photofragment kinetic energy balance and the radii of the CO^+ ion images. The (1−1) band of the CO E−X transition is also observed in this spectral region, and the separation of the blended spectrum into its (0−0) and (1−1) components can be enhanced by selective detection of different velocity components of the ion signals. The two-state mixing of C $^1\Sigma^+$ and E $^1\Pi$ states that accounts for the large Λ-doublet splitting in the E state is invoked to obtain the J-dependent mixing coefficients and effective line strengths for Q- and S-branch lines in section 3.3. Section 3.4 addresses the information carried in the overlapping and only partially resolved (0−0) and (1−1) bands of the E−X spectrum. The discussion of section 4 addresses the relative intensities of the other rotational branches, terminating in the f-symmetry component of the E state. While not as dramatic as the appearance of nominally forbidden transitions in the Q-branch, the R-branch intensities appear suppressed by about a factor of 3 relative to the S-branch intensities, but only at the high-J levels accessed in the OCS photodissociation. The selective suppression of ionization for the high-J, f-symmetry Λ components of the E $^1\Pi$ state suggests a previously unreported predissociation involving a $^1\Sigma^-$ state. We conclude with the prospects for future use of these transitions in photo-

DOI: 10.1021/acs.jpca.9b00109
J. Phys. Chem. A 2019, 123, 2780−2788

dissociation studies and extended spectroscopic investigations of the VUV states of CO.

2. EXPERIMENTAL SECTION

The molecular beam/velocity-map ion-imaging apparatus has been described in detail elsewhere.[44,45] In brief, the apparatus consists of three collinear regions containing the pulsed molecular beam source, the main interaction chamber, and the detector. During operation the source is evacuated by a diffusion pump and the other regions are each evacuated by a turbomolecular pump. Typical operating pressures are 1×10^{-4}, 2×10^{-6}, and 1×10^{-7} Torr, for the source, main, and detector regions, respectively. A General Valve series 9 pulsed valve produces a free jet expansion in the source region. The molecular beam is collimated by an electroformed skimmer between the source and main regions. In the main region, the laser beam intersects the molecular beam at 90°, photodissociating the OCS sample and ionizing CO photoproducts. Velocity mapping is accomplished using two Einzel lenses which accelerate the ions along the molecular beam axis, toward the detector region. The detector assembly consists of a pair of chevron microchannel plates (MCPs) and a P-47 phosphor screen. The signal from the phosphor screen was viewed by a Hamamatsu R928 photomultiplier tube for REMPI spectra, or by an IDS uEye gated CCD camera for images.

The sample through the pulsed nozzle was obtained by flowing He at a pressure of 1 atm through a bubbler of OCS maintained at 196 K, resulting in an OCS mole fraction of ~0.25. A single laser pulse was used to dissociate OCS and probe the nascent CO fragments. A Spectra Physics Pro-230-10 Nd:YAG was used to pump a Lambda Physik Scanmate dye laser to produce wavelengths ranging from 426 to 432 nm (Exalite/1,4-dioxane). The output was frequency doubled using a type I β barium borate crystal (BBO) and focused into the time-of-flight interaction region with a 250 mm focal length lens. The 213−216 nm light was linearly polarized parallel to the image plane and had pulse energies ranging from 0.5 to 3 mJ/pulse and an estimated UV line width of about 0.5 cm^{-1}. Dye laser frequency calibration was accomplished by reference to accurate CO X v = 0, J and CO E, v = 0, J term values tabulated in the recent atlas of Lemaire et al.[31]

3. RESULTS AND ANALYSIS

3.1. 2+1 E-X REMPI Spectra of CO. Previously reported REMPI spectra of room temperature samples of CO using the E−X transition[11,12] show the expected rotational structure of a $^1\Pi-^1\Sigma^+$ spectrum, with O- and P-branch lines extending to the red of the band origin, R- and S-branches shaded to the blue, and a weak Q-branch with intensity from only the lowest few rotational states. Figure 1 depicts the stick spectrum corresponding to a 300 K sample, for which the most probable rotational state is J = 7. In contrast, the photodissociation of OCS produces CO with a highly inverted rotational distribution,[1,3,4,8,46] peaked around J = 60, as depicted qualitatively in Figure 2. For this rotational distribution, one expects bandheads in the O- and P-branches, while the R- and S-branches consist of well-resolved lines. With normal two-photon line strength factors for a $^1\Pi-^1\Sigma^+$ transition, the Q-branch would be undetectable, but in Figure 2 the stick spectra are depicted with magnitudes derived only from lower state populations, for the sake of illustration.

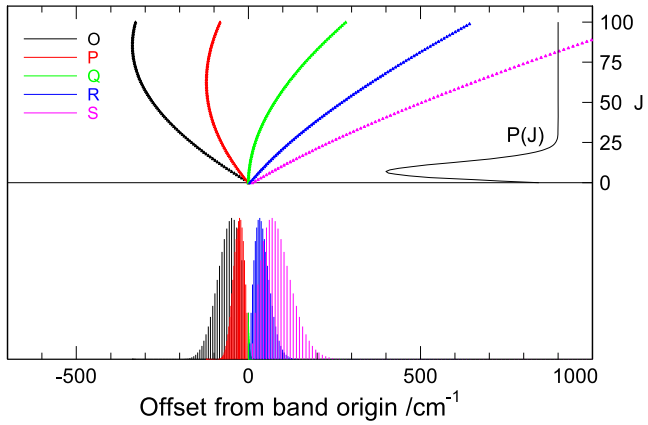

Figure 1. CO E−X stick spectrum and Fortrat parabolas for a 300 K thermal rotational distribution.

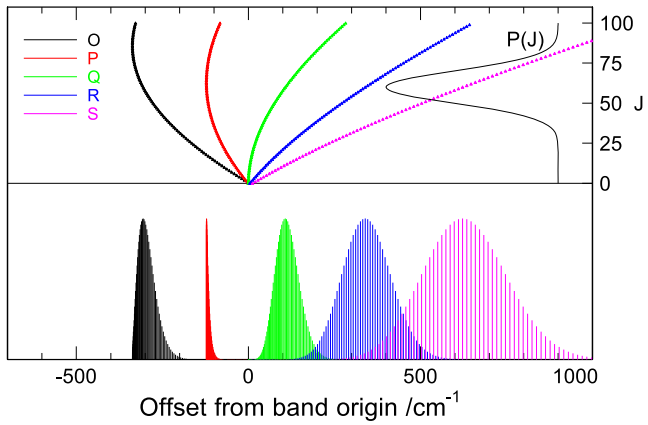

Figure 2. CO E−X stick spectrum and Fortrat parabolas for hot photofragment CO distribution. All rotational branches are depicted with amplitude derived only from lower state population, ignoring line strength factors.

From this figure, it can be seen that the R- and S-branches will be most useful for state-resolved ion imaging experiments, subject to such a rotational state distribution. In the two-photon transition, the S-, Q-, and O-branch lines sample the e-symmetry Λ-doublets, and the R- and P-branch lines sample the f-symmetry Λ-doublets. The E−X (1−1) band will have approximately the same structure, with an offset in the band origin of about 9.6 cm^{-1} to the blue. The (1−1) Franck−Condon factor is within a few percent of that for the (0−0) band,[1] as the potential energy curve for CO X $^1\Sigma^+$ is similar to that for the X $^2\Sigma^+$ state of CO^+ and its associated Rydberg states.[21]

Figure 3 shows the S-, Q-, and R-branches of the experimental spectrum, with rotational assignments for the (0−0) and (1−1) bands. The simulation will be discussed in section 3.3. The experimental REMPI spectrum is a composite of multiple shorter wavelengths scans, correcting for laser power and changes in the photodissociation cross section, although the latter effect was minimal. The vertical scaling of adjacent scan segments was adjusted to match the amplitudes of several common transitions shared by successive, overlapping scans.

The observation of transitions reaching higher rotational states of the E state of CO than have been previously reported

DOI: 10.1021/acs.jpca.9b00109
J. Phys. Chem. A 2019, 123, 2780−2788

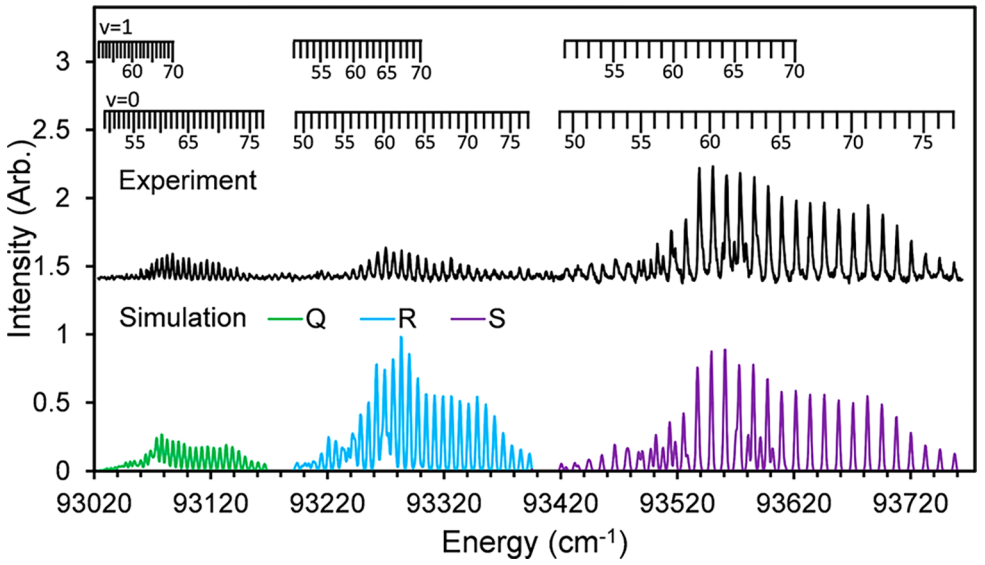

Figure 3. Q-, R-, S-branches of the (0−0) and (1−1) bands of the E-X 2+1 REMPI spectrum of CO. The *x*-axis is plotted in two photon energies. The experimental spectrum is shown on top (black). Simulated spectrum Q (green), R (blue), and S (purple) branches are shown below. The simulation is scaled to the S-branch experimental intensities.

provides an opportunity to compare the rotational energies of E-state "super-rotors"—states with rotational energies in excess of 10 000 cm^{-1}—with the predictions of molecular constants derived from accurate measurements of rotational levels restricted to less than half of that energy. Despite the long polynomial extrapolation, the high-J line positions predicted from the previously published effective rotational constants for the e- and f-symmetry components of the E state[18,24,47] are mutually consistent and within the approximately 0.5 cm^{-1} confidence limits of our newly measured values. A previous publication from this laboratory[1] reported inappropriately adjusted rotational constants and lacked an accurate dye laser calibration, although the correspondence between spectral features and line assignments was correct. After the dye laser calibration is corrected, previously published molecular constants for the v = 0 and v = 1 levels of the X and E states[47,48] are completely adequate to identify all the observed lines.

A particularly compelling case can be made for these Rydberg super-rotors as a laboratory for new examples of state mixing and perturbations in CO, as the very high angular momentum leads to strong enhancement of rotation-induced interaction matrix elements that are too small to matter in cold or thermal samples.

3.2. Kinetic Energy Measurements of CO Photofragments. The transitions now attributed to Q-branch transitions of the E−X (0−0) and (1−1) bands were not initially anticipated, due to our presumption of vanishing line strengths in the REMPI spectrum. A kinetic energy balance based on the photon energy, the ion image radius, and the putative assignment was thus used to verify the assignments. Similar methods have been described for pixel-to velocity calibration, or refinement of the bond dissociation energy of OCS in previous work.[3,5,8] Conservation of energy leads to the equation

$$E_{\text{available}} = h\nu - D_0 + E_{\text{OCS}} = E_{\text{CO}}(\text{v},J) + E_{\text{trans}} \quad (1)$$

where $h\nu$ is the photon energy, D_0 is the OCS dissociation energy for the S (^{1}D) + CO (v = 0, J = 0) pathway, E_{OCS} and E_{CO}(v, J) are the internal energies of the OCS precursor and CO photofragment, respectively, and E_{trans} is the total translational energy of the CO and S (^{1}D) photofragments. For jet-cooled OCS photodissociation precursor molecules, E_{OCS} can be neglected. At the highest rotational states measured there is a contribution from the ν_2 hotband but these features can be easily resolved from the signal originating from vibrationless OCS parent. Throughout the CO E−X spectral region, the mass 28 ion images display one or two rings of various radii, corresponding to the recoil velocities of CO (J) in v = 0 or v = 1, as the rotational transitions come into resonance. For the unambiguous S-branch transitions of the (0−0) band, the trend in measured radius with the CO rotational state permits a calibration of velocity to image pixel size, which can then be used to compute total translational energy of the putative Q-branch CO transitions. Using our spectral assignments along with rotational constants for X state v = 0 and v = 1, the internal energies of the CO photofragments could be calculated. Figure 4 shows a plot of the difference in energy between the photolysis photon energy and the calculated internal energy of the CO fragment versus the experimental translational energy for the transitions we

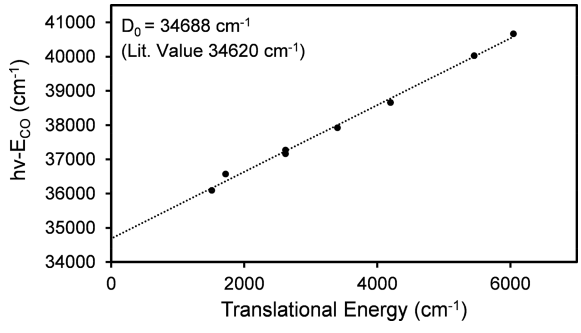

Figure 4. Translational energy analysis using experimentally derived speeds for v = 0 and v = 1 CO fragments using eq 1. The *y*-intercept of 34 688 cm^{-1} is consistent with previously reported values of D_0 for the S(^{1}D) channel.

DOI: 10.1021/acs.jpca.9b00109
J. Phys. Chem. A 2019, 123, 2780−2788

have assigned to Q-branch lines originating in v = 0, J = 55, 58, 64, 67, 70, 74 and v = 1, J = 61, and 64. A linear fit results in a slope of 0.97 ± 0.03 and the y-intercept of 34 688 cm^{-1}, in excellent agreement with the previously published D_0 for the S (^{1}D) channel of 34 620 cm^{-1},[3] supporting the assignment of the Q-branch.

3.3. C and E State Mixing: Λ-Doubling and Intensity Borrowing. For a quantitative estimate of the relative intensities of the nominally forbidden Q-branch and the fully allowed S-and O-branches, we consider the L-uncoupling interaction of the C and E states. The deperturbation analysis of Le Floch[19] used accurate experimental term values for the e- and f-symmetry levels of the CO E $^1\Pi$ state (v = 0), assuming the perturbation is only due to the nearby C $^1\Sigma^+$ state, the accurate term values of which have also been modified by the perturbation. The J-dependent mixing accounts for the Λ-doubling, and also the intensity borrowing that makes the two-photon Q-branch transitions visible. The f-symmetry energy levels of the E state are given by the unperturbed term values:

$$T(\mathrm{E}^1\Pi,\nu{=}0,J) = T_0^{\mathrm{E}} + B_0^{\mathrm{E}}(x-1) - D_0^{\mathrm{E}}(x-1)^2 \quad (2)$$

with $x = J(J+1)$, and the molecular constants, T, B, and D as tabulated by Le Floch.[19] The e-symmetry eigenvalues are the result of diagonalizing a 2 × 2 interaction matrix for the C state and the e-symmetry component of the E state. The diagonal matrix elements are

$$T(\mathrm{C}^1\Sigma,\nu{=}0,J) = T_0^{\mathrm{C}} + B_0^{\mathrm{C}}(x) - D_0^{\mathrm{C}}(x)^2 \quad (3)$$

and the unperturbed E-state term values are from eq 2. The off-diagonal rotation-electronic mixing is given by

$$\langle T(\mathrm{C}^1\Sigma,\nu{=}0,J)|\mathbf{H}^{\mathrm{RE}}|T(\mathrm{E}^1\Pi,\nu{=}0,J)^{\mathrm{e}}\rangle = 2\beta\sqrt{x} \quad (4)$$

with β a mixing parameter to be determined by fitting, along with the zero-order rotational constants for E and C states, in order to match the set of eigenvalues to the observed term values. The perturbed eigenstates are mixtures of the zero-order E and C states:

$$\psi_{\mathrm{E}} = \alpha_{\mathrm{E}}\psi_{\mathrm{E}}^0 + \alpha_{\mathrm{C}}\psi_{\mathrm{C}}^0 \quad (5)$$

where α_{E} and α_{C} are mixing coefficients in the E state eigenvector, normalized such that $|\alpha_{\mathrm{E}}|^2 + |\alpha_{\mathrm{C}}|^2 = 1$, and $|\alpha_{\mathrm{C}}|^2$ is a quantitative measure of the J-dependent Σ character of the e-symmetry E state levels. Note that this deperturbation approach gives zero-order rotational constants that are not identical to the effective B and D constants for the e- and f-symmetry levels of the E state, as was done in other analyses.[18,24,47]

E state term values up to J = 20 and C state term values up to J = 32 were used by Le Floch to determine zero-order molecular constants and the value of β = 1.735 cm^{-1}.[19] We have used these parameters to calculate the eigenvectors of the mixed C and E states at the higher rotational levels accessed from the OCS photofragments. For the rotational levels J < 30 used in the spectroscopic deperturbation analysis, the Σ character $|\alpha_{\mathrm{C}}|^2$ does not exceed 1%. However, the Σ character increases approximately quadratically with J, reaching 2% at J = 42, 4% at J = 61, and 6% at J = 76. The effective two-photon line strength for the E−X Q-branch at these high rotational levels is entirely derived from the C state character of the E state, $|\alpha_{\mathrm{C}}|^2$.

The trial simulation of the E−X REMPI spectrum shown at the bottom of Figure 3 was thus calculated, using v = 0 and v = 1 rotational state populations adapted from Wei et al.,[1] and a Q-branch line strength for a Σ−Σ transition times the J-dependent $|\alpha_{\mathrm{C}}|^2$ fractional weight, for both v = 0 and v = 1. The O- and S-branch line strengths will also be affected by the mixing of a small amount of a Σ−Σ path with the dominant Π−Σ path, with the possibility of interference. In this trial simulation, we have ignored any possible interference and computed a spectrum based on an incoherent sum of the similar line strength factors weighted by minor $|\alpha_{\mathrm{C}}|^2$ and dominant $|\alpha_{\mathrm{E}}|^2$ upper state characters. As the R- and P-branch transitions terminate on the f-symmetry level, pure Π−Σ line strengths were used in the trial simulation of these branches. The comparison of experimental and simulated spectra is presented in Figure 3. The relative intensities and contours of the S- and Q-branches are well reproduced in this simulation, where the visibility of the same e-symmetry levels is independent of J in the S-branch and quadratically increasing with J in the Q-branch. The R-branch, which terminates in the nominally unperturbed f-symmetry levels of the E state, is observed to be about 3 times weaker than the simulation. This relative suppression is not appreciably altered over the accessible range of laser intensities for which acceptable spectra could be recorded.

3.4. Comparisons of the (0−0) and (1−1) Bands. Previous work on the 214 nm photodissociation of OCS from this laboratory[1] reported CO rotational distributions in v = 0 and v = 1, and concluded that about 20% of the CO product was formed in v = 1 of the X state. This was based on the velocity distribution of S (^{1}D) products from ion imaging, combined with v = 0 and v = 1 rotational state distributions deduced from the interleaved S-branches of the (0−0) and (1−1) bands of the E−X REMPI spectrum. The relative REMPI intensities of the S-branches of the (0−0) and (1−1) bands agreed closely with the vibrational branching ratio deduced from the S (^{1}D) image. The CO internal energy distribution derived from the sulfur ion image cannot be affected by any differences in the CO absorption line strengths, Franck−Condon factors, predissociation, or partial saturation, leading to the conclusion that the absolute sensitivity for REMPI detection of the high rotational states of CO (X) v = 0 and v = 1 using the S-branches of the (0−0) and (1−1) E−X bands is similar.[1] In the present work, the relative intensities of the Q-branch lines in the interleaved (0−0) and (1−1) bands can be compared to the analogous S-branch lines to assess possible differences in the apparent rotational distributions and the apparent vibrational branching, as indicators of the J-dependent effective line strengths and any additional vibrational state dependence to the REMPI sensitivity. We anticipate no significant vibrational dependence to the mixing of the C and E states, as the electronic Σ/Π mixing is close to a classic "pure precession" mixing of the 3pπ and 3pσ Rydberg states,[49] for which the vibrational dependence should be minor. Indeed, the Λ-doubling q parameter in the E state v = 1 is 0.011 45(9) cm^{-1} compared to 0.011 82(3) in v = 0.[24] Accordingly, the simulation shown in Figure 3, with its expanded Q-branch region shown in Figure 5, has been computed with the same assumed J-dependent Q-branch line strengths derived from the Λ-doubling parameter for both v = 0 and v = 1 photoproducts. With no additional assumptions about the relative REMPI sensitivity of these two bands, the simulation of the interleaved Q-branch region is satisfactory, showing an enhancement in the relative intensity of the higher rotational lines compared to the S-branch spectra, and a similar

DOI: 10.1021/acs.jpca.9b00109
J. Phys. Chem. A 2019, 123, 2780−2788

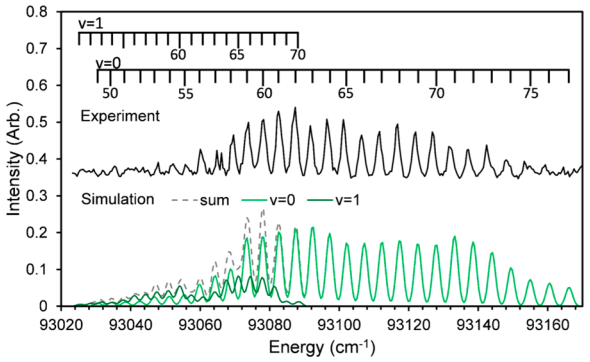

Figure 5. Expanded Q branch region of Figure 3. The *x*-axis is plotted in two photon energies. The experimental spectrum (black) is shown above, and the simulated spectrum is shown below, highlighting the decomposition into (0−0) and (1−1) branch lines.

apparent vibrational branching ratio in both S-branch and Q-branch regions.

As a check on the consistency of this partitioning of the blended spectrum into (0−0) and (1−1) contributions, images were taken at several wavelengths where Q lines of the (0−0) and (1−1) bands coincide, and the relative contributions of v = 0 and v = 1 fragments could be determined from the ion images. The inset in Figure 6 shows an image taken at 214.894

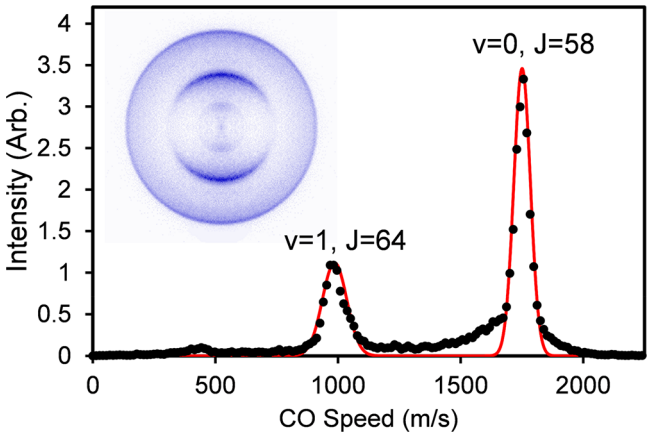

Figure 6. CO photofragment velocity distribution (black dots) and simulation (red line) at 214.894 nm, where the Q(58) and Q(64) lines of the (0−0) and (1−1) bands are simultaneously excited. The velocity distribution was extracted from the reconstruction of the ion image taken at 214.894 nm (shown in inset).

nm, where the Q(58) line of the (0−0) band and the Q(64) line of the (1−1) band are both resonantly excited. The polar onion peeling method was used to reconstruct the 3D fragment distribution from the 2D image.[50] The resulting angle-averaged 1D speed distribution is shown in Figure 6. The relative contributions of v = 0, J = 58 and v = 1, J = 64 can be determined by integrating the features in the speed distribution. The v = 0 and v = 1 features were fit with Gaussian functions, and the Gaussian peaks were integrated, yielding a v = 0 contribution of 68% and a v = 1 contribution of 32%. The decomposition of the REMPI spectrum into (0−0) and (1−1) contributions has the relative contributions at this wavelength of 73% and 27%. Comparable agreement was found for several other overlapped lines in the spectrum. The ion image analysis provides a consistency check on the decomposition of the REMPI spectrum into blended (0−0) and (1−1) contributions, supporting a common, J-dependent effective line strength function for the Q(0−0) and Q(1−1) bands. The similarity of the relative band intensities of the (0−0) to (1−1) REMPI spectra to the unbiased vibrational branching ratio based on the sulfur ion image suggests that the known differences in predissociation rates from v = 0 and v = 1 of the E state (at least at low rotational levels)[22,29] is insufficient to cause a difference in the REMPI intensities. The ratio of (1−1) to (0−0) intensities in the Q-branch, as in the S- and R-branches, showed no discernible dependence on the laser intensity for pulse energies between 0.5 and 3 mJ. This suggests that in this intensity range, which is on the order of 10^8 to 10^9 W/cm^2, the enhanced predissociation rates from the E state v = 1 levels compared to v = 0 are still insufficient to compete with a strongly saturated ionization step. This point is relevant to the discussion of section 4.2 below, where perturbation effects on the P- and R-branch intensities are considered.

4. DISCUSSION

4.1. Relative Branch Intensities: Q and S Branches. The relative strengths of the Q- and S-branches are satisfactorily modeled with a J-dependent state mixing of the e-symmetry levels, for both a thermal spectrum, where only the lowest J Q-branch lines are visible, and for the OCS photofragment spectrum, where the CO rotational distribution is dominated by very high rotational levels, between 40 and 80. The qualitative observation that the Q-branch becomes increasingly bright at high-J is well accounted for in this two-state mixing model. In retrospect, this is a natural consequence of the well-documented Λ-doubling mechanism, but we are unaware of previous examples of Q branch lines becoming bright at high rotational levels for a two-photon transition between $^1\Sigma^+$ and $^1\Pi$ states.

Hippler has described a type of interference effect in two-photon line strengths[51] that can lead to unexpected deviations from the line strengths originally given by Bray and Hochstrasser.[38] This discrepancy only applies to ΔΛ = 0 transitions for Λ > 0, for which the C $^2\Pi$−X $^2\Pi$ 2+1 REMPI spectrum of NO has been used as an example. This type of interference does not occur in a two-photon $^1\Pi-{}^1\Sigma^+$ transition, such as the CO E−X spectrum and cannot be the source of the anomalous intensities. The increasingly mixed character of the rotationally excited E state does allow for coherent mixtures of perpendicular $^1\Pi-{}^1\Sigma^+$ and parallel $^1\Sigma^+-{}^1\Sigma^+$ two-photon transition moments, with possible cross terms, which may play a role in modifying the S and O branch intensities, when both paths are allowed. The relatively small relative amplitude for the $^1\Sigma^+-{}^1\Sigma^+$ path limits the expected significance of this interference in the S and O branches, while the near zero contribution from the perpendicular path to the Q-branch makes the cross term negligible.

4.2. Relative Branch Intensities: P and R Branches. The one-photon E−X (0−0) spectrum shows a progressive enhancement of the P-branch lines relative to the R-branch lines at increasing J, with a complementary suppression of high-J P-branch lines relative to R in the C−X (0−0) band.[17] This can be described as an interference effect in the transition amplitudes caused by the J-dependent mixing of parallel and perpendicular transition moments, as described on page 388 of Lefebvre-Brion and Field.[34] In the one-photon spectrum, the P- and R-branches terminate in e-symmetry levels, the only

DOI: 10.1021/acs.jpca.9b00109
J. Phys. Chem. A 2019, 123, 2780−2788

ones that mix with the C $^1\Sigma^+$ state. This intensity anomaly is another face of the same e-symmetry mixing of $\Sigma^+-\Pi^+$ states that makes the two-photon Q-branch of the E−X spectrum bright at high-J.

In the two-photon E−X transition, P- and R-branch transitions terminate in the f-symmetry Λ-doublets of the E state, which are not subject to this rotationally mediated interaction with the C $^1\Sigma^+$ state. While appearing with normal intensities in the REMPI spectrum of thermal samples[11,12] the high-J lines of the R-branch observed in the one-laser OCS photodissociation experiment appear reduced in intensity by approximately a factor of 3 compared to the e-symmetry lines of the S-branch. A J-dependent loss of intensity in the R-branch lines should be detectable as a stronger suppression of the higher rotational states than the lower ones within the range of levels produced in the photodissociation. Such an apparent shift in the R-branch intensities to lower rotational levels than the S-branch intensity distribution is discernible, but subject to large uncertainties, due to the blending of (0−0) and (1−1) band lines and uncertainties associated with power normalization. The REMPI spectrum of room temperature samples of CO, in contrast, shows no strong branch-specific intensity deviations from unperturbed Π−Σ line strengths, apart from a weakly and uniformly suppressed S-branch intensity, and some intensity and wavelength-dependent effects attributed to secondary photodissociation of the CO^+ ion signals.[11,12] Our measurements of P- and O-branch intensities for the high rotational states are subject to the uncertainty of comparing strong, unresolved O- and P-branch bandheads with the much weaker, resolved lines of Q-, R-, and S-branches. It appears, however, that the P-branch signals for the OCS photoproduct rotational states are similarly suppressed compared to the anticipated spectral intensity relative to the O-branch using unperturbed line strengths.

The suppression of high-J R- (and P-) branch intensities relative to both low-J R-branch intensities and relative to high-J S-branch intensities encourages us to consider specific perturbations of the f-symmetry Λ component of the E state. Only a perturbing state of $^1\Sigma^-$ symmetry will selectively affect the higher rotational levels of f-symmetry in a $^1\Pi$ state. The I $^1\Sigma^-$ state of CO is the lowest energy state of this symmetry, correlating to ground-state atomic states O (^{3}P) + C (^{3}P), with a dominant electronic configuration $(1\sigma)^2(2\sigma)^2(3\sigma)^2(4\sigma)^2(5\sigma)^2(1\pi)^3(2\pi)^1$: a valence $\pi^3\pi^*$ state. The I state is known from direct absorption in the quadrupole-allowed I $^1\Sigma^-$−X $^1\Sigma^+$ transitions in the vacuum ultraviolet[52] and through localized perturbations in the A $^1\Pi$ state (v = 0) near J = 50, giving intensity to the perturbing f-symmetry levels.[53] The I state is unbound at the energy of the E state (v = 0), so one should not expect strong level shifts from the mixing of E $^1\Pi$ (f) levels with the I $^1\Sigma^-$ continuum, but the perturbation could cause a reduction in absorption intensity by mixing with the dark state, and/or a reduction in the CO^+ signal by enhancing the predissociation rate in competition with the ionization step. The interaction of narrow with broad perturbing levels is discussed on pages 672−683 of ref 34, where the possibility of strong intensity anomalies without significant frequency shifts is pointed out.

One problem with this explanation for the reduced intensity of high rotational levels of f-symmetry in the E $^1\Pi$ state is that the dominant electronic configuration at the E state vibrational minimum is $...4\sigma^2 5\sigma^1 1\pi^4 3\pi^1$, featuring a Rydberg 3p$\pi$ electron.[54] This electron configuration differs by more than a single spin orbital from that of the I $^1\Sigma^-$ state, making the electronic-rotational coupling weak. Two plausible explanations can be considered. The strong coupling observed for the e-symmetry interaction of C and E states mixes states which primarily differ in the 3pσ vs 3pπ Rydberg electron, added to the $^2\Sigma^+$ CO^+ core. An analogous perturbation by a Rydberg $^1\Sigma^-$ state derived from the $...4\sigma^2 5\sigma^2 1\pi^3 3\pi^1$ configuration would be a possible mechanism, for which the coupled states differ only in the X $^2\Sigma^+$ vs the A $^2\Pi$ CO^+ core. To our knowledge, this $^1\Sigma^-$ Rydberg state has not previously been characterized. The perturbations would closely resemble the mixing known between the X $^2\Sigma^+$ and A $^2\Pi$ states of CO^+. If this $^1\Sigma^-$ Rydberg state is responsible for the selective high-J perturbation of f-symmetry Λ-doublets, one may also expect interaction with the isoconfigurational $^1\Delta$ Rydberg state to affect both e- and f-symmetry Λ components at high J.

A second plausible mechanism is perturbation by the I $^1\Sigma^-$ valence state, mediated by the E′ $^1\Pi$ state, which provides partial valence character to the primarily Rydberg E $^1\Pi$ state. The outer well of the E/E′ state is described[27] by a mixture of two dominant valence electronic configurations: $...(4\sigma)^2(1\pi)^3(5\sigma)^1(2\pi)^2$ and $...(4\sigma)^1(1\pi)^4(5\sigma)^2(2\pi)^1$. The first is isoconfigurational with the k $^3\Pi$ state, which allows the indirect spin−orbit perturbations of the E state to occur by means of its partial E′ valence character.[23,25] The second dominant configuration differs by a single spin−orbital from the valence I $^1\Sigma^-$ with its configuration $...4\sigma^2 1\pi^3 5\sigma^2 2\pi^1$. Configuration interaction that mixes valence character from the E′ into the E state could account for a homogeneous electronic-rotational mixing of the high-J f-symmetry component of the E state by the I $^1\Sigma^-$ state. Further *ab initio* study would be appropriate to investigate these possibilities.

Even with a plausible candidate for perturbing the f levels of the E state, there are unconfirmed quantitative details. The complete mixing of a bright level with a single dark state can cause at most a 50% reduction of the absorption intensity, seemingly insufficient to account for a 3-fold reduction, as discussed on p 371 of ref 34. The attribution of the reduced intensity to enhanced predissociation rates is also problematic. If an enhanced predissociation rate were to be the cause of the reduced intensity of high-J R-branch lines, one would also expect to see a reduced sensitivity to CO v = 1 when observed through the (1−1) band of the E−X transition, since predissociation from v = 1 in the E state is known to be about 10 times faster than from v = 0, at least for low and moderate rotational states.[16,22,29] Instead, the uncorrected relative intensities of the (0−0) and (1−1) bands in Q-, R-, and S-branches all appear to be consistent with the branching ratio of CO photoproducts produced in v = 1 and v = 0, as independently derived from the sulfur ion image at a similar excitation wavelength near 214 nm, which has no spectroscopic bias for the CO fragment states.[1] One might hope to verify the kinetic effect of predissociation in competition with ionization, as has been done, for example, on isolated rotational predissociations characterized by Baker et al.[12] The suppression of ionization through the $J_e = J_f = 6$ states of the E state v = 0 in $^{13}C^{16}O$, for example, was found to be strongly enhanced at low laser powers relative to nearby unperturbed levels, even as the spectral shift associated with the perturbation was too small to measure. Cassiani et al.[24] have pointed out the challenges of quantitative interpretation of the suppression of REMPI intensities in terms of predissociation rates under tight focusing conditions and we

DOI: 10.1021/acs.jpca.9b00109
J. Phys. Chem. A 2019, 123, 2780−2788

concur. Unfortunately, the usable dynamic range for intensity-dependent measurements is restricted in these one-color experiments, where the same laser produces and probes the photofragments, and nonresonant background at mass-to-charge 28 raises the minimum laser intensity required for high-quality spectra. With a measured intensity dependence over a wider range, it might be possible to clarify the possible role of differential saturation that presently eludes us. Furthermore, if enhanced predissociation accounts for the reduced REMPI intensities, there should be an incremental line broadening of the R-branch two-photon lines compared to S- or Q-branch REMPI transitions at these high rotational levels. All of the transitions we have observed are limited by laser bandwidth, power broadening and Doppler broadening at the high photofragment velocities, making such a predicted incremental lifetime broadening unobservable by our measurements.

5. CONCLUSION

Anomalous Q-branch intensity has been observed in the E−X 2+1 REMPI spectrum of highly rotationally excited CO fragments arising from the photodissociation of OCS around 214 nm. The assignment of the Q-branch has been confirmed through velocity mapped ion imaging experiments. The observed Q-branch intensity is well described by a *J*-dependent linear combination of Σ−Σ and Σ−Π line strengths, with weights directly derived from the Λ-doubling parameter that characterizes the mixing of the E $^1\Pi$ state with the nearby C $^1\Sigma^+$ state. The apparent suppression of the P- and R-branches, which should be unaffected by the C state mixing, provides a tantalizing hint of previously unobserved perturbations by a $^1\Sigma^-$ state, but remains currently unconfirmed.

AUTHOR INFORMATION

Corresponding Author

*E-mail: swnorth@tamu.edu.

ORCID

G. E. Hall: 0000-0002-8534-9783

R. W. Field: 0000-0002-7609-4205

S. W. North: 0000-0002-0795-796X

Notes

The authors declare no competing financial interest.

ACKNOWLEDGMENTS

The work at Texas A&M University was supported by the Robert A. Welch Foundation (A-1405). The contributions to this work by GEH were carried out at Brookhaven National Laboratory under Contract No. DE-SC0012704 with the U.S. Department of Energy, Office of Science and supported by its Division of Chemical Sciences, Geosciences, and Biosciences within the Office of Basic Energy Sciences. R.W.F. thanks the National Science Foundation [Grant number CHE-1800410] for support of his research, which includes substantive collaborations. The authors thank Professor W. Wei for experimental assistance and insightful discussions. Helpful discussions with Professor T. J. Sears are gratefully acknowledged.

REFERENCES

(1) Wei, W.; Wallace, C. J.; McBane, G. C.; North, S. W. Photodissociation dynamics of OCS near 214 nm using ion imaging. *J. Chem. Phys.* **2016**, *145* (2), 024310.

(2) Sun, Z.-F.; Scheidsbach, R. J. A.; Suits, A. G.; Parker, D. H. Imaging multiphoton ionization and dissociation of rotationally warm CO via the B $^1\Sigma^+$ and E $^1\Pi$ electronic states. *J. Chem. Phys.* **2017**, *147* (1), 013906.

(3) van den Brom, A. J.; Rakitzis, T. P.; Janssen, M. H. M. State-to-state photodissociation of carbonyl sulfide (ν_2 = 0,1|J|M). II. The effect of initial bending on coherence of S(D21) polarization. *J. Chem. Phys.* **2005**, *123* (16), 164313.

(4) Sato, Y.; Matsumi, Y.; Kawasaki, M.; Tsukiyama, K.; Bersohn, R. Ion imaging of the photodissociation of OCS near 217 and 230 nm. *J. Phys. Chem.* **1995**, *99* (44), 16307−16314.

(5) Komissarov, A. V.; Minitti, M. P.; Suits, A. G.; Hall, G. E. Correlated product distributions from ketene dissociation measured by dc sliced ion imaging. *J. Chem. Phys.* **2006**, *124* (1), 014303.

(6) Liu, J.; Wang, F.; Wang, H.; Jiang, B.; Yang, X. A velocity map ion-imaging study on ketene photodissociation at 208 and 213nm: Rotational dependence of product angular anisotropy. *J. Chem. Phys.* **2005**, *122* (10), 104309.

(7) Sutradhar, S.; Samanta, B. R.; Samanta, A. K.; Reisler, H. Temperature dependence of the photodissociation of CO2 from high vibrational levels: 205−230 nm imaging studies of CO($X^1\Sigma^+$) and O(^{3}P, ^{1}D) products. *J. Chem. Phys.* **2017**, *147* (1), 013916.

(8) van den Brom, A. J.; Rakitzis, T. P.; Heyst, J. v.; Kitsopoulos, T. N.; Jezowski, S. R.; Janssen, M. H. M. State-to-state photodissociation of OCS (ν_2 = 0,1|J|M). I. The angular recoil distribution of CO (X $^1\Sigma^+$;v = 0|J). *J. Chem. Phys.* **2002**, *117* (9), 4255−4263.

(9) Spiglanin, T. A.; Perry, R. A.; Chandler, D. W. Internal state distributions of CO from HNCO photodissociation. *J. Chem. Phys.* **1987**, *87* (3), 1568−1576.

(10) Fujii, A.; Ebata, T.; Ito, M. Production of rotationally state selected ions by resonant enhanced multiphoton ionization of CO in a supersonic free jet. *Chem. Phys. Lett.* **1989**, *161* (2), 93−97.

(11) Hines, M. A.; Michelsen, H. A.; Zare, R. N. 2+1 resonantly enhanced multiphoton ionization of CO via the E $^1\Pi$−X $^1\Sigma^+$ transition: From measured ion signals to quantitative population distributions. *J. Chem. Phys.* **1990**, *93* (12), 8557−8564.

(12) Baker, J.; Lemaire, J. L.; Couris, S.; Vient, A.; Malmasson, D.; Rostas, F. A 2+1 REMPI study of the E-X transition in CO. Indirect predissociations in the E 1Π state. *Chem. Phys.* **1993**, *178* (1), 569−579.

(13) Wurm, S.; Feulner, P.; Menzel, D. Resonance-enhanced multiphoton ionization spectroscopy of X $^1\Sigma^+$ and a $^3\Pi$ carbon monoxide using electron stimulated desorption as a source for rovibronically excited species. *J. Chem. Phys.* **1996**, *105* (16), 6673−6687.

(14) Wei, W.; Wallace, C. J.; Grubb, M. P.; North, S. W. A method of extracting speed-dependent vector correlations from 2+1 REMPI ion images. *J. Chem. Phys.* **2017**, *147* (1), 013947.

(15) Tilford, S. G.; Vanderslice, J. T.; Wilkinson, P. G. High-resolution vacuum ultraviolet absorption spectrum of the E $^1\Pi$←X $^1\Sigma^+$ transition in CO. *Can. J. Phys.* **1965**, *43* (3), 450−456.

(16) Letzelter, C.; Eidelsberg, M.; Rostas, F.; Breton, J.; Thieblemont, B. Photoabsorption and photodissociation cross sections of CO between 88.5 and 115 nm. *Chem. Phys.* **1987**, *114* (2), 273−288.

(17) Stark, G.; Heays, A. N.; Lyons, J. R.; Smith, P. L.; Eidelsberg, M.; Federman, S. R.; Lemaire, J. L.; Gavilan, L.; de Oliveira, N.; Joyeux, D.; Nahon, L. High-resoution oscillator strength measurements of the v′=0,1 bands of the B-X, C-X and E-X systems in five isotopologues of carbon monoxide. *Astrophys. J.* **2014**, *788* (1), 67.

(18) Amiot, C.; Roncin, J. Y.; Verges, J. First observation of the CO E $^1\Pi$ to B $^1\Sigma^+$ and C $^1\Sigma$ + to B $^1\Sigma^+$ band systems. Predissociation in the E $^1\Pi$(v = 0) level. *J. Phys. B: At. Mol. Phys.* **1986**, *19* (1), L19.

(19) Le Floch, A. Accurate energy levels for the C1Σ+ (v = 0) and E1Π (v = 0) states of 12C16O. *J. Mol. Spectrosc.* **1992**, *155* (1), 177−183.

(20) Lee, L. C.; Guest, J. A. Quantitative absorption and fluorescence studies of CO from 1060 to 1550 Å. *J. Phys. B: At. Mol. Phys.* **1981**, *14* (18), 3415.

DOI: 10.1021/acs.jpca.9b00109
J. Phys. Chem. A 2019, 123, 2780−2788

(21) Ciocca, M.; Kanik, I.; Ajello, J. M. High-resolution studies of extreme-ultraviolet emission from CO by electron impact. *Phys. Rev. A: At., Mol., Opt. Phys.* **1997**, *55* (5), 3547−3556.
(22) Ubachs, W.; Velchev, I.; Cacciani, P. Predissociation in the E $^1\Pi$, v = 1 state of the six natural isotopomers of CO. *J. Chem. Phys.* **2000**, *113* (2), 547−560.
(23) Lefebvre-Brion, H.; Majumder, M. Isotopic dependence of the predissociations of the E$^1\Pi$ state of CO. *J. Chem. Phys.* **2015**, *142* (16), 164306.
(24) Cacciani, P.; Hogervorst, W.; Ubachs, W. Accidental predissociation phenomena in the E $^1\Pi$, v = 0 and v = 1 states of $^{12}C^{16}O$ and $^{13}C^{16}O$. *J. Chem. Phys.* **1995**, *102* (21), 8308−8320.
(25) Majumder, M.; Sathyamurthy, N.; Vazquez, G. J.; Lefebvre-Brion, H. Interpretation of the accidental predissociation of the E $^1\Pi$ state of CO. *J. Chem. Phys.* **2014**, *140* (16), 164303.
(26) Vázquez, G. J.; Amero, J. M.; Liebermann, H. P.; Lefebvre-Brion, H. Potential Energy Curves for the $^1\Sigma$+ and $^{1,3}\Pi$ States of CO. *J. Phys. Chem. A* **2009**, *113* (47), 13395−13401.
(27) Lefebvre-Brion, H.; Liebermann, H. P.; Vazquez, G. J. An interpretation of the anomalous $^1\Pi$ vibronic structure in the far-UV spectrum of CO. *J. Chem. Phys.* **2010**, *132* (2), 024311.
(28) Lefebvre-Brion, H.; Lewis, B. R. Comparison between predissociation mechanisms in two isoelectronic molecules: CO and N_2. *Mol. Phys.* **2007**, *105* (11−12), 1625−1630.
(29) Cacciani, P.; Ubachs, W.; Hinnen, P. C.; Lyngå, C.; Huillier, A. L.; Wahlström, C. G. Lifetime Measurements of the E$^1\Pi$, v = 0 and v = 1 States of 12C16O,13C16O, and 13C18O. *Astrophys. J.* **1998**, *499* (2), L223.
(30) Ubachs, W.; Eikema, K. S. E.; Levelt, P. F.; Hogervorst, W.; Drabbels, M.; Meerts, W. L.; ter Muelen, J. J. Accurate determination of predissociation rates and transition frequencies for CO. *Astrophys. J.* **1994**, *427*, L55−L58.
(31) Lemaire, J. L.; Heays, A. N.; Eidelsberg, M.; Gavilan, L.; Stark, G.; Federman, S. R.; Lyons, J. R.; de Oliveira, N. Atlas of new and revised high-resolution spectroscopy of six CO isotopologues in the 101−115 nm range. *Astron. Astrophys.* **2018**, *614*, A114.
(32) Visser, R.; van Dishoeck, E. F.; Black, J. H. The photo-dissociation and chemistry of CO isotopologues: applications to interstellar clouds and circumstellar disks*. *Astron. Astrophys.* **2009**, *503* (2), 323−343.
(33) Daprà, M.; Niu, M. L.; Salumbides, E. J.; Murphy, M. T.; Ubachs, W. Constraint on a Cosmological Variation in the Proton-to-electron Mass Ratio from Electronic CO Absorption. *Astrophysical Journal* **2016**, *826* (2), 192.
(34) Lefebvre-Brion, H.; Field, R. W. *The Spectra and Dynamics of Diatomic Molecules*, revised and enlarged ed.; Elsevier, 2004.
(35) Eikema, K. S. E.; Hogervorst, W.; Ubachs, W. Predissociation Rates in Carbon-Monoxide - Dependence on Rotational State, Parity and Isotope. *Chem. Phys.* **1994**, *181* (1−2), 217−245.
(36) Gao, H.; Song, Y.; Chang, Y. C.; Shi, X. Y.; Yin, Q. Z.; Wiens, R. C.; Jackson, W. M.; Ng, C. Y. Branching Ratio Measurements for Vacuum Ultraviolet Photodissociation of (CO)-C-12-O-16. *J. Phys. Chem. A* **2013**, *117* (29), 6185−6195.
(37) Hines, M. A.; Zare, R. N. The interaction of CO with Ni(111): Rainbows and rotational trapping. *J. Chem. Phys.* **1993**, *98* (11), 9134−9147.
(38) Bray, R. G.; Hochstrasser, R. M. Two-photon absoption by rotating diatomic molecules. *Mol. Phys.* **1976**, *31* (4), 1199−121.
(39) Hay, S.; Shokoohi, F.; Callister, S.; Wittig, C. Collisional metastability of high rotational states of CN ($X\ ^2\Sigma^+$, $v'' = 0$). *Chem. Phys. Lett.* **1985**, *118* (1), 6−11.
(40) Karczmarek, J.; Wright, J.; Corkum, P.; Ivanov, M. Optical centrifuge for molecules. *Phys. Rev. Lett.* **1999**, *82* (17), 3420−3423.
(41) Villeneuve, D. M.; Aseyev, S. A.; Dietrich, P.; Spanner, M.; Ivanov, M. Y.; Corkum, P. B. Forced molecular rotation in an optical centrifuge. *Phys. Rev. Lett.* **2000**, *85* (3), 542−545.
(42) Murray, M. J.; Ogden, H. M.; Toro, C.; Liu, Q. N.; Mullin, A. S. Impulsive Collision Dynamics of CO Super Rotors from an Optical Centrifuge. *ChemPhysChem* **2016**, *17* (22), 3692−3700.
(43) Milner, V.; Hepburn, J. W. Laser Control of Ultrafast Molecular Rotation. *Advances in Chemical Physics, Vol 159* **2016**, *159*, 395−412.
(44) Tokel, O. *Photodissociation and O(^{1}D) Reactions of Nitrous Oxide*; Cornell University, 2011.
(45) Wei, W. *Vector correlations and their applications in photo-dissociation dynamics study*; Texas A&M University, 2017.
(46) Sivakumar, N.; Hall, G. E.; Houston, P. L.; Hepburn, J. W.; Burak, I. State-resolved photodissociation of OCS monomers and clusters. *J. Chem. Phys.* **1988**, *88* (6), 3692−3708.
(47) Cacciani, P.; Ubachs, W. High resolution study of Q-branches in the E$^1\Pi$−X$^1\Sigma$+ (0,0) band of $^{12}C^{16}O$, $^{13}C^{16}O$, and 13C18O. *J. Mol. Spectrosc.* **2004**, *225* (1), 62−65.
(48) Guelachvili, G.; Devilleneuve, D.; Farrenq, R.; Urban, W.; Verges, J. Dunham Coefficients for 7 Isotopic-Species of CO. *J. Mol. Spectrosc.* **1983**, *98* (1), 64−79.
(49) Mulliken, R. S.; Christy, A. Λ-Type Doubling and Electron Configurations in Diatomic Molecules. *Phys. Rev.* **1931**, *38* (1), 87−119.
(50) Roberts, G. M.; Nixon, J. L.; Lecointre, J.; Wrede, E.; Verlet, J. R. R. Toward real-time charged-particle image reconstruction using polar onion-peeling. *Rev. Sci. Instrum.* **2009**, *80* (5), 053104.
(51) Hippler, M. Interference in two-photon rotational line strengths of diatomic molecules. *Mol. Phys.* **1999**, *97* (1−2), 105−116.
(52) Herzberg, G.; Simmons, J. D.; Bass, A. M.; Tilford, S. G. The forbidden I $^1\Sigma$−−X $^1\Sigma^+$ absorption bands of carbon monoxide. *Can. J. Phys.* **1966**, *44* (12), 3039−3045.
(53) Le Floch, A. C.; Launay, F.; Rostas, J.; Field, R. W.; Brown, C. M.; Yoshino, K. Reinvestigation of the CO A$^1\Pi$ state and its perturbations: The v = 0 level. *J. Mol. Spectrosc.* **1987**, *121* (2), 337−379.
(54) Cooper, D. L.; Kirby, K. Theoretical study of low-lying $^1\Sigma^+$ and $^1\Pi$ states of CO. I. Potential energy curves and dipole moments. *J. Chem. Phys.* **1987**, *87* (1), 424−432.

DOI: 10.1021/acs.jpca.9b00109
J. Phys. Chem. A 2019, 123, 2780−2788